

## WAVELET MULTI-RESOLUTION ANALYSIS FOR THE LOCAL SEPARATION OF MICROGRAVITY ANOMALIES AT ETNA VOLCANO

Filippo Greco<sup>(1)</sup>, Gilda Currenti<sup>(1)</sup>, Ciro Del Negro<sup>(1)</sup>, Agnese Di Stefano<sup>(1,2)</sup>, Rosalba Napoli<sup>(1)</sup>, Antonio Pistorio<sup>(1,2)</sup>, Danila Scandura<sup>(1,3)</sup>, Gennaro Budetta<sup>(1)</sup>, Maurizio Fedi<sup>(4)</sup>

<sup>(1)</sup> Istituto Nazionale di Geofisica e Vulcanologia, Sezione di Catania, Italy

<sup>(2)</sup> Dipartimento di Ingegneria Elettrica, Elettronica e dei Sistemi, Università degli Studi di Catania, Italy

<sup>(3)</sup> Dipartimento di Matematica e Informatica, Università degli Studi di Catania, Italy

<sup>(4)</sup> Dipartimento di Scienze Della Terra, Università degli Studi di Napoli “Federico II”, Italy

greco@ct.ingv.it

### Abstract

A microgravity 14-year-long data set (October 1994–September 2007) recorded along a 24-kilometer East-West trending profile of 19 stations was analyzed to detect underground mass redistributions related to the volcanic activity involving the southern flank of Mt. Etna volcano (Italy). An important issue with the above data-set is the need of separating the useful signal (i.e. the volcano-related one) from unwanted components (instrumental, human-made, seasonal and other kinds of noise). To filter the gravity data-set from these last components we propose the wavelet multi-resolution analysis. This method provides a good separation of the long period component from the short period one, and allows exploring the local features of the signal with a detail matched to their characteristic scale. Using the discrete wavelet transform (DWT), the gravity data are decomposed into a low-resolution approximation level and several detail levels. Once the useful signal has been suitably separated from the noise, the residual space-time-image evidences, over the studied area and time-interval, (i) recurrences in both space (i.e. zones under which mass redistributions occur more frequently) and time (i.e. cyclic processes) and (ii) microgravity anomalies correlated with the ensuing volcanic activity.

### Key words

Microgravity, Volcano monitoring, Etna volcano.

### 1 Data analysis and results

The East-West profile (Fig. 1), because of the more frequent measurements and the high station density (almost 1 station/km), provides the core microgravity data

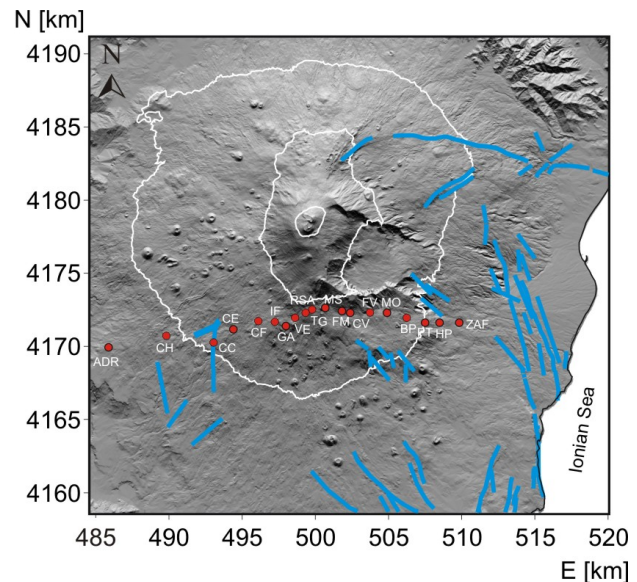


Figure 1. Sketch map of Mt. Etna showing the gravity stations (red circles) that compose the East-West profile on the southern slope of the volcano which runs from Zafferana to Adrano across the Rifugio Sapienza. The blue lines show the major surface fault systems bordering the eastern and southern sectors of the volcano. Geographical coordinates are expressed in UTM projection, zone 33N.

for Etna. Since its installation (summer of 1994), 96 surveys were carried out and a large data-set, spanning a 14-year long period (1994–2007), was collected using the Scintrex CG-3M gravimeter (serial # 9310234). Figure 2 shows the gravity variations measured in the East-West profile stations (y axis) between October 1994 and September 2007 (x axis).

The space-time map shows significant gravity in-

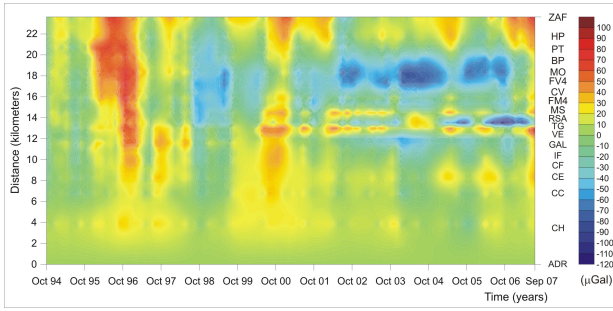


Figure 2. Image showing the space/time gravity variations along a 24-kilometer East-West trending profile of 19 stations between October 1994 and September 2007. All measurements were referred to the outermost station of the profile (Adrano; ADR). The error on temporal gravity differences along the East-West profile is  $10 \mu\text{Gal}$ .

crease/decrease cycles, with different wavelengths, reaching the maximum amplitude of approximately  $110 \mu\text{Gal}$ . The main gravity cycles are concentrated along the central and eastern limb of the profile [Greco et al., 2009]. Besides useful signal (i.e. the volcano-related one), the gravity map includes unwanted components (instrumental, human-made, seasonal and other kinds of noise). In order to filter the gravity data-set from these last components the wavelet multi-resolution analysis was applied. The wavelet analysis provides a good separation of the long period component from the short period one, and allows exploring the local features of the signal with a detail matched to their characteristic scale. Using the discrete wavelet transform (DWT), the gravity data are decomposed into a low-resolution approximation level and several detail levels [Fedi and Quarta, 1998; Fedi and Florio, 2003]. The detail levels can be regarded as the difference of information between the approximations of the signal at subsequent scales. In a two-dimensional multiresolution process three detail levels can be obtained along horizontal, vertical and diagonal directions at each scale [Fedi and Florio, 2003]. We are particularly interested in the horizontal and vertical components that reflect temporal and spatial gravity variations, respectively. The space-time matrix consists of  $50 \times 100$  grid data at about 500 m step and with a 1.5 month average sampling. The multiresolution analysis decomposes the data from the finest to the coarsest levels, corresponding to level  $\ell = -(L-1)$  and  $\ell = 0$ , respectively, where  $L = \log_2(m)$  for discrete data of  $m$  values. In the case of a 2D multiresolution analysis  $m$  is the minimum size of the data matrix dimension. For the considered gravity data-set the finest level is at most  $\ell = -5$ .

Several wavelet bases may be, however, taken into consideration to compute the DWT. The ‘‘Minimum Entropy Criterion’’ (MEC) was used to evaluate a compactness measure, which estimates how the signal energy can be substantially assembled in few components [Coifman and Wickerhauser, 1993; Fedi and Quarta,

1998]. Using this criterion, the entropy of the wavelet coefficients for various types of wavelet basis may be determined, and the optimal wavelet basis may be chosen as the one giving the minimum entropy value. The Shannon's entropy was calculated for several wavelet basis over the wavelet coefficients from level  $\ell = 0$  to  $\ell = -5$ , and ranges between 3.14 and 4.50 (Table 1), with the minimum value obtained for the Symlet 4 basis. The wavelet decomposition of gravity data set by Symlet 4 gives one low-resolution approximation map and five total detail maps with the most energetic levels from  $\ell = -1$  to  $\ell = -5$  (Fig. 3). The  $D_{-5}$  detail map (Fig. 3) evidences the presence of local noise at VE and TG stations situated at the central part of the profile, very close to the Rifugio Sapienza (Fig. 1). Indeed, these stations are often affected by a human-made noise due to the presence of tourist facilities. The high resolution map of the  $D_{-4}$  detail shows up short-wavelength time-space gravity variations (Fig. 3). Most of the signal in the horizontal components of the  $D_{-4}$  detail map can be associated to quite shallow sources which produce localized gravity anomaly. Besides the presence of high frequency components in the horizontal details, seasonal variations come up in the vertical details of the  $D_{-4}$  and  $D_{-3}$  maps (Fig. 3). A late-winter maximum and a late-summer minimum is observed with amplitude ranges between  $\pm 40 \mu\text{Gal}$  peak-to-peak in the easternmost stations of the profile. These gravity changes are consistent with water-table fluctuations. A gravity change of about  $\pm 20 \mu\text{Gal}$ , corresponding to water-table fluctuations of 3.5 - 5 m and an effective porosity of the aquifer in the range 0.09 to 0.14 [Aureli, 1973], was evaluated by Budetta et al. [1999] using average values estimated from only the western stations data (from CH to TG; Fig. 1). The DWT analysis evidences that seasonal variations induce local effects at each gravity station. Different fluctuations in the underground water-table depend on climate, weather, and geological setting around the gravity station and the related gravity effect can differ from station to station in magnitude and temporal dependence. Higher gravity variations are observed on the eastern part. Indeed, yearly rainfall data show high precipitation value on the eastern flank with a precipitation ratio of about two with respect to the westernmost flank [SIAS, 2007]. In addition, the stations located in the westernmost tip of the profile are very close to the extended outcrops of the sedimentary substrate [Romano, 1982]. The substrate serves as a seal along the base of the fractured and vesicular volcanic sequence, and hence the Etna's aquifers are confined mostly to volcanic rock [Ogniben, 1966]. Accordingly, only restricted aquifers are located near the westernmost stations (Fig. 1), where any gravity change due to water-table fluctuations can be then considered meaningless. Once the wavelet analysis was performed and gravity data were suitably filtered from the (i) noise ( $D_{-5}$ ), (ii) the effect of sources very close to the surface ( $D_{-4}$ ), and (iii) seasonal components due to water-table fluctuations ( $D_{-3}$  and  $D_{-4}$ ),

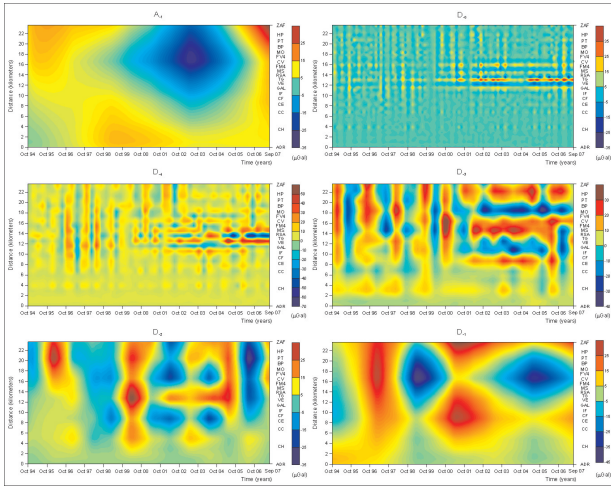


Figure 3. Wavelet multiresolution analysis of the 14-year-long gravity data-set. Using a Symlet 4 wavelet base, five total detail maps and a low resolution map ( $A_1$ ) were obtained. The meaningful gravity anomalies are related to the total detail levels from  $D_{-3}$  to  $D_{-1}$ .

the gravity residual can be attributed to subsurface bulk density (Fig. 4). Since the vertical components  $D_{-3}$  and  $D_{-4}$  contain gravity variations with a period of about one year, the filtering procedure unfortunately could remove useful signal with similar temporal scale. Thus, in the following we consider only gravity variations with period longer than one year.

The residual gravity map shows long period gravity increase and decrease cycles with duration ranges between a few years and several years, and with a wavelength of order of 10-12 km (Fig. 4). The gravity increase/decrease cycles affect mainly the central and eastern stations of the profile, whereas the gravity changes at stations closest to the reference station (ADR) remain within  $20 \mu\text{Gal}$  during the entire period (Fig. 4). A first complete gravity increase/decrease cycle attains a maximum amplitude of approximately  $90 \mu\text{Gal}$ , which started during the early months of 1995 (gravity increase), culminated at the end of 1996, and continued until late-1998 (gravity decrease), when the mean value of gravity at each station reached a level lower than it was in 1994-95, before the increase took place (Fig. 4). The considerable increase/decrease of gravity field recorded in this period (late-1995 to late-1998) is among the largest ever recorded along the profile until now.

A second increase/decrease gravity cycle, affecting the same stations of the previous one, but mostly evident in the central portion of the profile, was observed between mid-1999 (gravity increase), culminating at the mid-2000 (maximum amplitude about  $80 \mu\text{Gal}$ ) and continuing until early-2004. The 1999-2000 gravity increase was interrupted by a progressive gravity decrease of about  $80 \mu\text{Gal}$ , which started between early-2001, continued very slowly until early-2004, and partially compensated for the previous gravity increase.

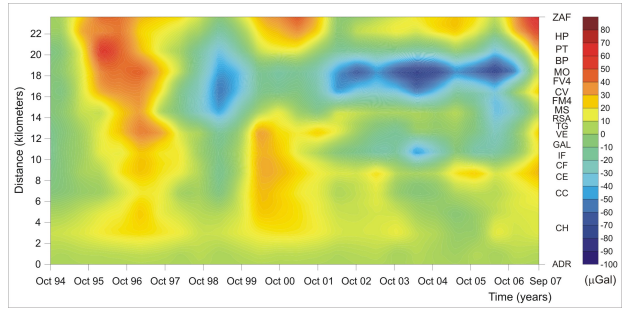


Figure 4. The 14-year-long gravity data-set after filtering the contributions identified in the  $D_{-5}$  and  $D_{-4}$  total maps and the  $D_{-3}$  vertical detail.

Table 1. Shannon's entropy values relative to wavelet basis. The minimum entropy values is obtained using Symlet 4 bases.

Wavelet Basis	Shannon's Entropy
Coiflet 2	3.24
Coiflet 3	3.97
Coiflet 4	4.50
Daubechies 1	4.38
Daubechies 2	3.60
Daubechies 3	4.02
Daubechies 4	3.20
Symmlet 1	4.38
Symmlet 2	3.60
Symmlet 3	4.02
<b>Symmlet 4</b>	<b>3.14</b>
Symmlet 5	3.55
Symmlet 6	3.83
Symmlet 7	3.81

After the 2001 no significant gravity increase/decrease cycles, in terms of both amplitude and wavelength, occurred. Moreover, the gravity field on the easternmost stations shows a persistent negative gravity anomaly during the period 2001-2006, whereas the gravity in the western flank is almost unchanged. After about 5 years of absence of significant gravity cycles, a new semi-cycle with characteristics similar to the previous ones seems to start at the end of 2006 and continues during the survey carried out in September 2007.

## 2 Conclusion

The analysis of long-period microgravity observations demonstrated that in the last 14 years just two (mid-1995 to mid-1998 and late-1999 to late-2001) major episodes of magma intrusion occurred beneath the

southern sector of the volcano in the shallow storage zone. Another mass accumulation in the shallow plumbing system of the volcano started in late 2006 and was still in progress in September 2007. We are confident that the frequent and regular surveys of the East-West gravity profile indicate possible magma rising months to years before the onset of a new Etna's eruption.

## References

- Aureli, A. (1973). *Idrogeologia del fianco occidentale etneo*, 2° Convegno Internazionale sulle Acque Sotterranee, Palermo, pp. 425–486.
- Budetta, G., D. Carbone, and F. Greco (1999). *Subsurface mass redistributions at Mount Etna (Italy) during the 1995-96 explosive activity detected by microgravity studies*, Geoph. J. Int. 138, pp. 77–88.
- Coifman, RR and M.V. Wickerhauser (1993). *Wavelets and adapted waveform analysis. A toolkit for signal processing and numerical analysis*, Proceedings of Symposia in Applied Mathematics 47, pp. 119–145.
- Greco, F., Currenti, G., Del Negro, C., Napoli, R., Scandura, D., Budetta, G., Fedi, M., Boschi, E. (2009). *Space-time gravity variations to look deep into the southern flank of Etna volcano*, J. Geophys. Res., submitted.
- Fedi, M. and G. Florio (2003). *Decorrelation and removal of directional trends of magnetic fields by the wavelet transform: application to archaeological areas*, Geoph. Prospect. 51, pp. 261–272.
- Fedi, M. and T. Quarta (1998). *Wavelet analysis for the regional-residual and local separation of potential field anomalies*, Geoph. Prospect. 46, pp. 507–525.
- Ogniben, L. (1966). *Lineamenti idrogeologici dell'Etna*, Rivista Mineraria Siciliana pp. 100–102, 1–24.
- Regione Siciliana - SIAS - Servizio Informativo Agrometeorologico Siciliano.
- Romano, R. (1982). *Geological map of Mt. Etna*, Progetto Finalizzato Geodinamica, Istituto Internazionale di Vulcanologia, Catania, 1:50.000 scale.